ARTICLE

OBC
www.rsc.org/obc

From 1D strands to extended molecular assemblies in the binary compounds of dithiooxamide and dithiobiurea with crown ethers

Yurii A. Simonov,[a] Marina S. Fonari,*[a] Michael J. Zaworotko,[b] Heba Abourahma,[b] Janusz Lipkowski,[c] Edward V. Ganin[d] and Arkadii A. Yavolovskii[e]

[a] *Institute of Applied Physics Academy of Sciences of Moldova, Chisinau, Moldova. E-mail: fonari.xray@phys.asm.md; Fax: (373 2) 72 58 87; Tel: (373 2) 73 81 54*

[b] *Department of Chemistry, University of South Florida, 4202 East Fowler Avenue (SCA400), Tampa, Florida, 33620*

[c] *Institute of Physical Chemistry Polish Academy of Sciences, Warsaw, Poland*

[d] *Odessa State Environmental University of the Ministry of Education and Science of Ukraine, Odessa, Ukraine*

[e] *Bogatsky Physico-Chemical Institute, National Academy of Sciences of Ukraine, Odessa, Ukraine*

Received 4th February 2003, Accepted 26th June 2003
First published as an Advance Article on the web 11th July 2003

The hydrogen-bonding networks for seven new binary compounds of dithiooxamide, $(NH_2CS)_2$ (**dtox**) and dithiobiurea $(NH_2CSNH)_2$ (**dtur**) with crown ethers, 18-crown-6 (18C6), 15-crown-5 (15C5), 12-crown-4 (12C4), *cis–syn–cis–* (DCHA), and *cis–anti–cis–* (DCHB) isomers of dicyclohexyl-18-crown-6 are discussed. (15C5·**dtox**), (18C6·**dtur**) and (DCHB·**dtur**) afford one-dimensional hydrogen-bonded polymeric arrays where the components alternate. In (DCHA ·**2dtox**) and (DCHB ·**2dtox**) the similar hydrogen-bonded chains are further interlinked *via* **dtox** molecules to generate layered motifs. In (15C5·**2dtur**) the **dtur** molecules are self-assembled into layers *via* N–H ··· S hydrogen bonds. 15C5 spacers link adjacent layers into a three-dimensional network. In (12C4·**dtur**) the **dtur** molecules are arranged in chains. These chains alternate with the crown molecules attached to them through N–H ··· O hydrogen bonds in such a way that each 12C4 appears to be linked with four **dtur** molecules and *vice versa* thus providing a three-dimensional grid.

The last decade has witnessed tremendous advances in the understanding of, and the ability to manipulate, molecular and supramolecular assemblies.[1] There are new paradigms concerning the design and synthesis of a new generation of functional materials and molecules. Such advances are a consequence of the fundamental importance of intermolecular interactions, structure and cooperativity in many aspects of molecular science, from environmental science to molecular biology, pharmacology, and materials science. Thus, the prospects for control and manipulation of materials at the molecular level, particularly in areas related to non-covalent bonding and nanotechnology, are now truly exceptional.

Crystal engineering[2] is predicated on the assumption that crystals are *de facto* examples of self-assembly, *i.e.* crystals are comprised from a series of molecular recognition events or *supramolecular synthons*.[3] It also offers a more realizable goal than crystal structure prediction since it relies on design and allows for careful selection of substrates, *i.e.* substances that are predisposed to form predictable self-assembled superstructures can be targeted for study. Furthermore, the prototypal molecules used in crystal engineering contain *exofunctional molecular recognition sites* and they can be complementary with themselves (self-assembly)[4] or with other molecules (modular self-assembly).[5] Coincidentally, most pharmaceutical or biologically important molecules also contain exterior molecular recognition sites and, although this makes them susceptible to polymorphism and solvate formation, it also makes them attractive candidates for crystal engineering studies. The ability of crystalline self-assemblies to be built from a bottom-up approach[6] could provide an exceptional control of the design of new phases at a molecular level.

Supramolecular chemistry through hydrogen bonding is a driving force for the formation of binary compounds involving crown ethers. Our longstanding interest in multiply H–bonded complexes has aimed at utilizing the small biologically important organic molecules, rich in both H–donor and acceptor groups, in the construction of supramolecular networks with classic crown molecules. We have used hydrogen bonds successfully in purely organic crystals to build one-dimensional motifs (chains), and two-dimensional motifs (sheets).[7] Although the host–guest chemistry of 18-crown-6 (host) and its substituted analogues[8] has been widely studied, less success has been achieved in the design of diverse supramolecular architectures in the complexes based on 12-crown-4[9] and 15-crown-5.[10] Molecular complexes of 18-crown-6 with urea, thiourea and their derivatives have previously been reported.[11] The availability of two amine groups in the urea and thiourea molecules provides an opportunity for interactions with the crown molecule in addition to the self-assembly interactions of these small molecules *via* N–H ··· O or N–H ··· S hydrogen bonding. The dithiooxamide (**dtox**) $(NH_2CS)_2$ and dithiobiurea (**dtur**) $(NH_2CSNH)_2$ represent suitable candidates for building of supramolecular architectures as they contain H-bond donor groups (NH_n, n = 1, 2) and H-bond acceptor groups (S atoms). The crystal structures of pure **dtox**[12] and pure **dtur**[13] reveal three-dimensional networks being sustained by intermolecular N–H ··· S interactions.

We report herein the hydrogen-bonding organization and the specific features of supramolecular architectures for seven new binary compounds (Scheme 1), **dtox** with 15-crown-5 (15C5), (complex **1**, ratio 1 : 1), **dtox** with *cis–syn–cis* isomer of dicyclohexyl-18-crown-6 (DCHA), (**2**, ratio 1 : 2), **dtox** with *cis–anti–cis* isomer of dicyclohexyl-18-crown-6 (DCHB), (**3**, ratio 1 : 2); **dtur** with 18-crown-6 (18C6), (**4**, ratio 1 : 1), **dtur** with DCHB (**5**, ratio 1 : 1), **dtur** with 15C5 (**6**, ratio 1 : 2), and **dtur** with 12-crown-4 (12C4), (**7**, ratio 1 : 1) elucidated by conventional chemical methods (^{1}H, ^{13}C NMR and TGA) and X-ray crystal structure analysis, see Experimental.

DOI: 10.1039/b301379k

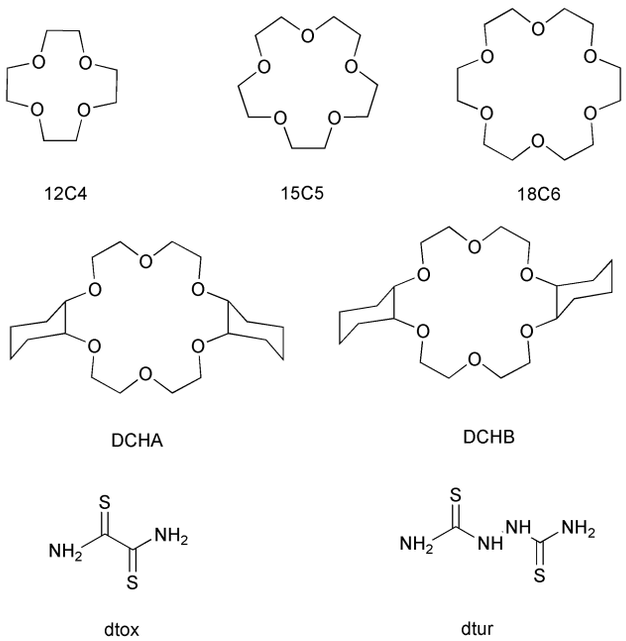

Scheme 1

Two crystalline complexes of **dtox** with benzo-5-crown-5 (B15C5), (ratio 1 : 1)[10a] and 18C6 (ratio 1 : 2)[14] were reported. In the former structure B15C5 and **dtox** molecules alternate in the chains due to N–H ··· O interactions. In the latter one, four **dtox** molecules are attached to each 18C6 and bridge four additional crown ligands *via* N–H ··· O hydrogen bonds. The alternating 18C6–**dtox** hydrogen-bonding chains are combined into a two-dimensional grid through N–H ··· S interactions. The different structural types exhibited by the system **dtox**–crown molecule provoked us to continue the study of possible supramolecular patterns in the assemblies of **dtox** with a symmetrically mismatched 15C5 molecule and with two dicyclohexyl derivatives of 18C6, DCHA and DCHB, having a restricted flexibility of the 18-membered macrocycle in comparison with the 18C6 counterpart.

Complexes of dithiooxamide with crown ethers

The ORTEP drawing for (**1**) is shown in Fig. 1. 15C5·**dtox** (**1**) crystallises in the triclinic *P*-1 space group and contains one crown and one **dtox** molecule per asymmetric unit (Fig. 1). The **dtox** molecule is disordered in two positions, **A** and **B**, with probabilities of 59.22(7) and 40.78(6)%, respectively. We will only discuss the **A** position of the **dtox** molecule, while Table 1 contains the hydrogen-bonding parameters for both positions.

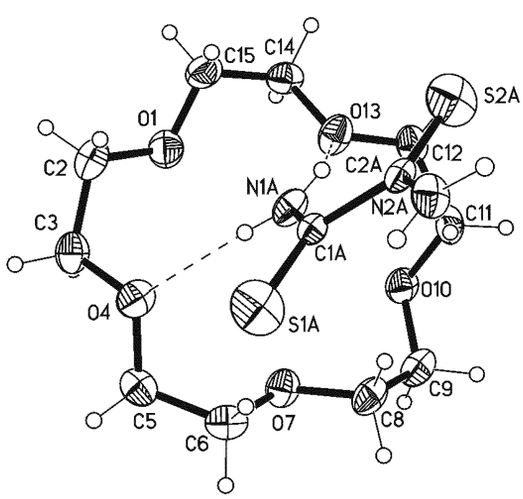

Fig. 1 ORTEP drawing for (**1**). The thermal ellipsoids are given with 30% probability level. Only one of two disordered positions are given for the **dtox** molecule.

The molecules in (**1**) are arranged in a T-shape mode with the dihedral angle between the mean plane of crown oxygen pentagon and the planar skeleton of **dtox** molecule equal to 78.7(5)°. Each **dtox** molecule bridges two adjacent 18C6 molecules translated along the *a* axis *via* two hydrogen bonds with the participation of both of the terminal amine groups, N(1A) ··· O(13) 2.98(3), N(1A) ··· O(4) 2.97(3) Å, and N(2A) ··· O(7) (x + 1, y, z) 3.07(2), N(2A) ··· O(10) (x + 1, y, z) 2.85(2) Å. The neighbouring non-centrosymmetric chains are related by an inversion centre in the crystal (Fig. 2).

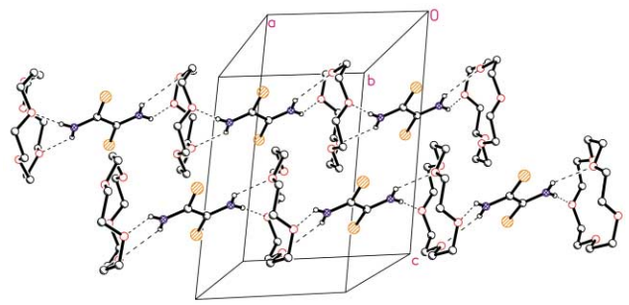

Fig. 2 Arrangement of chains in (**1**). Red: oxygens, blue: nitrogens, orange: sulfurs.

The organisation of (**1**) is similar to the complex B15C5·**dtox**.[10b] It means that the phenyl substituent influences the final architecture to a minor extent. To the best of our knowledge, it is the second example after the system of 15-membered crown ether, 15C5, B15C5–3,4-diamino-1,2,5-oxadiazole[10c] which also shows the closeness of supramolecular organization (the molecules are also arranged into the alternate chains *via* N–H ··· O hydrogen bonds).

(**2**) crystallises in the monoclinic space group *C*2/*c*. The asymmetric unit contains half of crown molecule and two halves of two crystallographically non-equivalent **dtox** molecules. The ORTEP diagram for (**2**) is shown in Fig. 3.

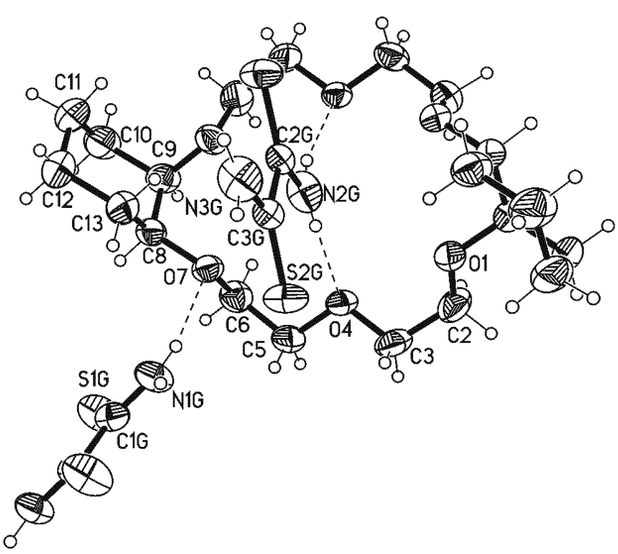

Fig. 3 ORTEP drawing for (**2**). The thermal ellipsoids are given with 50% probability level. Only one position is given for the **dtox** molecule.

DCHA and one of two **dtox** molecules (defined by the S(2G) atom and named here as **dtox2**) reside on a two-fold axis, while the second **dtox** molecule (defined by S(1G) atom and named here as **dtox1**) occupies the position around an inversion centre. The **dtox2** molecule is disordered and only one position is shown in the figures and further discussed. Two **dtox** molecules feature different structural functions in the supramolecular

Table 1 Intermolecular hydrogen bonds in (**1**)–(**7**)

D–H ··· A	*d*(H ··· A)/Å	*d*(D ··· A)/Å	∠(DHA)/°	Symmetry code for acceptor
(**1**)				
N(1a)–H(1Na) ··· O(13)	2.30	2.98(3)	136	*x, y, z*
N(1a)–H(1Nb) ··· O(4)	2.12	2.97(3)	174	*x, y, z*
N(2a)–H(2Na) ··· O(7)	2.58	3.07(2)	117	$x + 1, y, z$
N(2a)–H(2Nb) ··· O(10)	2.12	2.85(2)	143	$x + 1, y, z$
N(1b)–H(1Nc) ··· O(10)	2.48	2.93(3)	113	$x + 1, y, z$
N(1b)–H(1Nd) ··· O(7)	2.15	2.96(4)	157	$x + 1, y, z$
N(2b)–H(2Nc) ··· O(4)	2.50	3.14(3)	132	*x, y, z*
N(2b)–H(2Nd) ··· O(13)	2.05	2.89(4)	165	*x, y, z*
(**2**)				
N(1G)–H(1Nb) ··· O(7)	2.13(2)	2.994(2)	169(2)	*x, y, z*
N(2G)–H(2N) ··· O(4)	2.36(2)	3.107(2)	160(3)	*x, y, z*
N(3G)–H(3N) ··· O(4)	2.12(3)	2.938(2)	166(3)	$x, y - 1, z$
(**3**)				
N(1G)–H(2G1) ··· O(1)	2.20(2)	3.039(2)	164(2)	$-x + 1, -y + 1, -z$
N(2G)–H(1G2) ··· O(4)	2.18(2)	2.985(2)	163(2)	*x, y, z*
N(2G)–H(1G2) ··· O(7)	2.56(2)	3.100(2)	124(2)	*x, y, z*
N(2G)–H(2G2) ··· O(4)	2.28(2)	2.984(2)	144(2)	$-x + 1, -y + 1, -z$
(**4**)				
N(1G)–H(2N1) ··· O(1)	2.23(2)	3.056(2)	164(2)	*x, y, z*
N(1G)–H(1N1) ··· O(7)	2.15(2)	3.007(2)	165(2)	*x, y, z*
N(2G)–H(1N2) ··· O(13)	2.28(2)	2.982(2)	147(2)	$x, y - 1, z$
N(3G)–H(1N3) ··· O(16)	2.22(2)	2.932(2)	151(2)	*x, y, z*
N(4G)–H(1N4) ··· O(4)	2.38(2)	3.163(2)	160(2)	$x, y - 1, z$
N(4G)–H(2N4) ··· O(10)	2.20(2)	3.058(2)	166(2)	$x, y - 1, z$
(**5**)				
N(1G)–H(1N1) ··· O(4)	2.26(4)	3.091(2)	150(4)	*x, y, z*
N(1G)–H(2N1) ··· O(13)	2.43(4)	3.213(3)	149(3)	*x, y, z*
N(2G)–H(1N2) ··· O(7)	2.03(3)	2.855(2)	166(2)	$x, y - 1, z$
N(3G)–H(1N3) ··· O(13)	2.19(4)	2.946(3)	151(3)	*x, y, z*
N(4G)–H(1N4) ··· O(16)	2.11(3)	2.961(2)	163(2)	$x, y - 1, z$
N(4G)–H(2N4) ··· O(4)	2.11(3)	2.941(2)	157(3)	$x, y - 1, z$
(**6**)				
N(3G)–H(3GA) ··· S(1G)	2.47(2)	3.334(2)	170(2)	$-x + 1/2, y - 1/2, z$
N(2G)–H(2GA) ··· S(2G)	2.47(2)	3.297(2)	161(2)	$-x + 1/2, y + 1/2, z$
N(4G)–H(4GA) ··· S(1G)	2.53(2)	3.396(2)	172(2)	$-x, y - 1/2, -z + 1/2$
N(4G)–H(4GB) ··· S(2G)	2.72(2)	3.464(1)	142(2)	$-x, y + 1/2, -z + 1/2$
N(1G)–H(1GA) ··· O(4)	2.25(3)	2.940(3)	141(3)	*x, y, z*
N(1G)–H(1GA) ··· O(1)	2.58(3)	3.093(3)	121(2)	$-x, -y, -z$
N(1G)–H(1GB) ··· O(7)	2.08(2)	2.859(3)	151(2)	$-x, -y, -z$
N(1G)–H(1GB) ··· O(13)	2.18(2)	2.891(3)	141(2)	*x, y, z*
(**7**)				
N(1G)–H(7N) ··· O(7a)	1.95(2)	2.833(2)	171(2)	$-x, -y + 1, -z + 2$
N(1G)–H(8N) ··· O(10)	1.99(2)	2.842(2)	153(2)	$-x, -y + 1, -z + 1$
N(2G)–H(9N) ··· S(2G)	2.37(2)	3.275(2)	169(2)	$x, -y + 3/2, z + 1/2$
N(3G)–H(10N) ··· S(1G)	2.36(2)	3.252(2)	170(2)	$x, -y + 3/2, z - 1/2$
N(4G)–H(11N) ··· O(1)	2.19(2)	2.976(2)	161(2)	*x, y, z*
N(4G)–H(12N) ··· O(10a)	2.20(2)	2.991(2)	172(2)	$x, y, z - 1$
N(11G)–H(1N) ··· O(4)	1.99(2)	2.860(2)	170(2)	*x, y, z*
N(11G)–H(2N) ··· O(1a)	2.02(2)	2.864(2)	158(2)	*x, y, z*
N(12G)–H(3N) ··· S(12G)	2.44(2)	3.326(2)	169(2)	$x, -y + 3/2, z - 1/2$
N(13G)–H(4N) ··· S(11G)	2.37(2)	3.235(2)	170(2)	$x, -y + 3/2, z + 1/2$
N(14G)–H(5N) ··· O(7)	2.08(2)	2.953(2)	170(2)	$-x + 1, -y + 1, -z + 2$
N(14G)–H(6N) ··· O(4a)	2.08(2)	2.955(2)	161(2)	$-x + 1, -y + 1, -z + 2$

organisation. DCHA and **dtox2** alternate in the chains running along the *b* direction in the unit cell. The dihedral angle between the mean planes of planar framework of the **dtox2** molecule and the six oxygens of DCHA is 65.13(2)°. The **dtox2** molecule situated on the proximal face of DCHA affords two equal hydrogen bonds with the central oxygen atoms of the crown molecule, N(2G) ··· O(4) 3.107(2) Å. From the rear face of the same crown molecule the next **dtox2** molecule participates by N(3G) functionality in the H-bonding with the same oxygen atoms N(3G) ··· O(4) (x, $y - 1$, z) 2.938(2) Å. The **dtox1** molecule bridges the neighbouring center-of-symmetry related chains *via* one single N–H ··· O hydrogen bond, N(1G) ··· O(7) 2.994(2) Å providing the layer that is developed in the *ab* plane (Fig. 4).

The layer is built of the centrosymmetric cages that unite four crown and four **dtox** molecules in an alternative mode, each cage being closed by 12 N–H ··· O hydrogen bonds. Two crystallographically different **dtox** molecules are arranged in such a way that the dihedral angle between the mean planes of their non-hydrogen skeletons is 56.87(5)°. The arrangement of the components in the two-dimensional grid makes it impossible for sulfur atoms to participate in any self-assembled

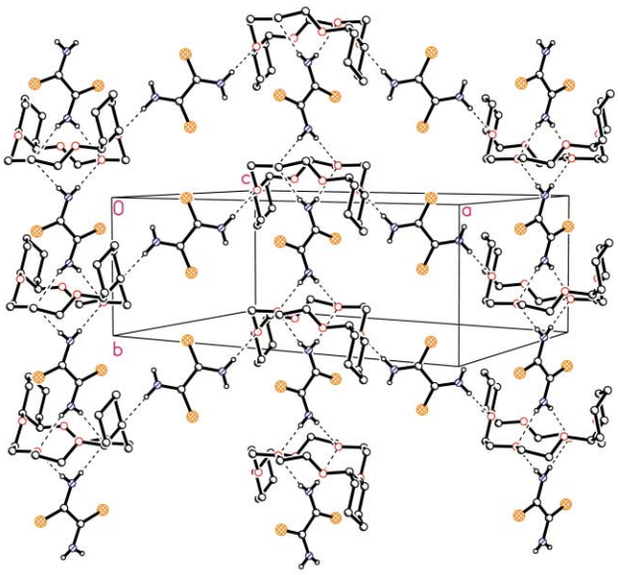

Fig. 4 View of the layer in (**2**). Red: oxygens, blue: nitrogens, orange: sulfurs.

N–H · · · S contacts found both in the structure of **dtox**[12] itself and in its complex with 18C6.[14]

(**3**) crystallises in monoclinic space group $P2_1/n$ with the asymmetric unit cell containing half of the crown molecule and two halves of two crystallographically independent **dtox** molecules, all residing on inversion centres. The ORTEP diagram for (**3**) is shown in Fig. 5.

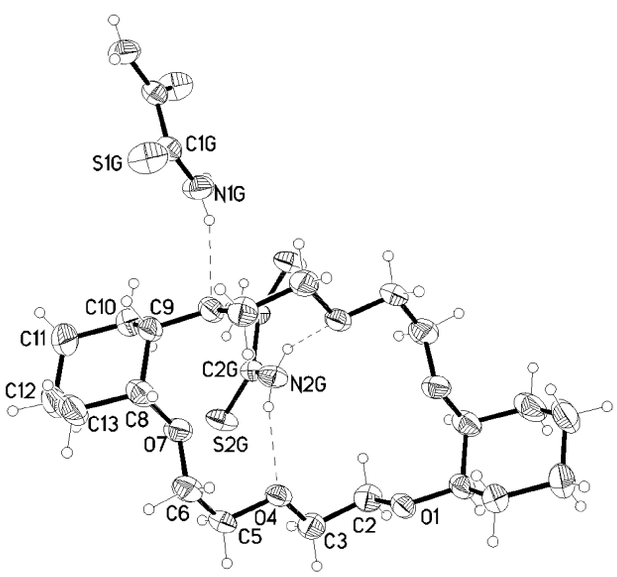

Fig. 5 ORTEP drawing for (**3**). The thermal ellipsoids are given with 50% probability level.

The two types of **dtox** molecules are arranged in perfectly the same way as in (**2**), with the dihedral angle between the mean planes of their skeletons equal to 56.68(6)°. The packing motif in (**3**) is similar to that of (**2**). DCHB and **dtox2** molecules alternate in a chain running along the *b* direction. Due to the inversion centre, each **dtox2**–DCHB–**dtox2** associate in the chain is stabilised by four center-of-symmetry-related N–H · · · O hydrogen bonds with the central oxygen atoms of the crown molecule, N(2G) · · · O(4) 2.985(2) and N(2G) · · · O(4) ($-x + 1, -y + 1, -z$) 2.984(2) Å. The same donor centre is involved in a subsidiary N–H · · · O interaction, N(2G) · · · O(7) 3.100(2) Å. The dihedral angle between the mean planes of the framework of the **dtox2** molecule and six oxygen atoms of the crown cavity is 72.42(6)°. **Dtox1** molecules bridge neighbouring chains *via* two equal N–H · · · O bonds, N(1G) · · · O(1) ($-x + 1, -y + 1, -z$) 3.039(2) Å, to generate layers that propagate parallel to the *ab* plane (Fig. 6).

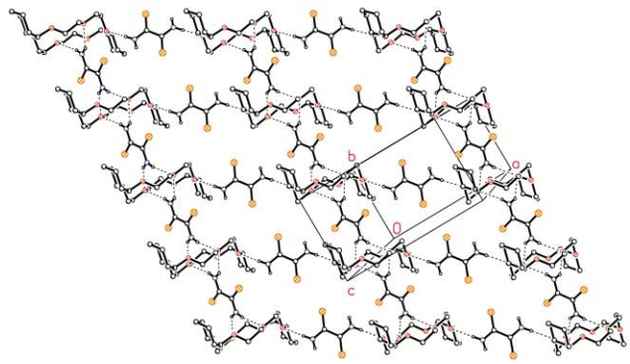

Fig. 6 View of the layer in (**3**). Red: oxygens, blue: nitrogens, orange: sulfurs.

To the best of our knowledge, this is the first example where two isomers of DCH18C6 yielded two supramolecular architectures of such pronounced similarity. It is evident that the dimensionality of **dtox** species is the crucial factor that dictates the similar arrangement of the components in the complexes with a minor influence arisen from the orientation of the cyclohexyl substituents. In the other known pairs, the clathrates of two isomers of DCH18C6 with malononitrile,[15a] zwitter-ion of amidosulfuric acid, $NH_3^+SO_3^-$,[15b] 3,5-dichlorobenzenesulfamide,[15c,d] 4-aminobenzenesulfamidine,[15e] 4-methylbenzenesulfamide,[15f] different supramolecular motifs have always been found for clathrates with the same guest.

Complexes of dithiobiurea with crown ethers

(**4**) is depicted in Fig. 7, it crystallizes with a 1 : 1 ratio of components in monoclinic space group $P2_1/c$ containing one 18C6 and one **dtur** molecule per asymmetric unit.

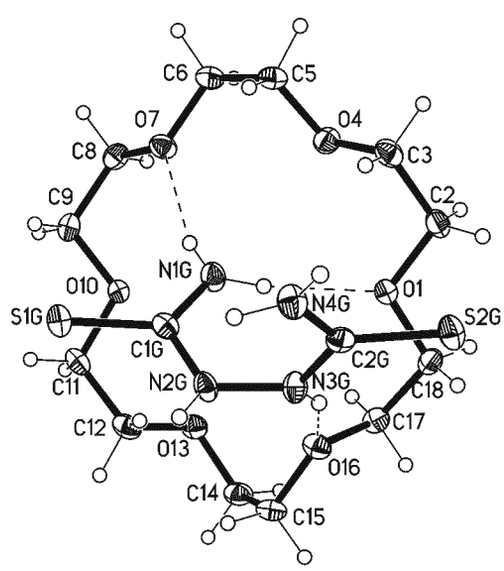

Fig. 7 ORTEP drawing for (**4**). The thermal ellipsoids are given with 50% probability level.

The molecules are held together by N–H · · · O hydrogen bonds with the participation of terminal and central amine groups of **dtur** in a twisted mode. The amine group defined by the N(1G) atom provides two hydrogen bonds with the crown oxygens, N(1G) · · · O(1) 3.056(2), N(1G) · · · O(7) 3.007(2) Å. The secondary amine group, defined by the N(3G) atom, provides a single hydrogen bond on the same face of the crown

molecule, N(3G) ··· O(16) 2.932(2) Å. The terminal amine group, defined by the N(4G) atom and secondary amine group, defined by the N(2G) atom, afford in a similar fashion N–H ··· O hydrogen bonds to the next crown molecule, N(4G) ··· O(4) (x, $y-1$, z) 3.163(2), N(4G) ··· O(10) (x, $y-1$, z) 3.058(2), N(2G) ··· O(13) (x, $y-1$, z) 2.982(2) Å, generating a chain running along the b direction in the unit cell (Fig. 8). Thus, all H-acceptors (crown oxygen atoms) and all H-donors (amine groups) are involved in N–H ··· O interactions. Sulfur atoms do not contribute to any hydrogen-bonding interactions. The chains are packed in a centrosymmetric mode in the crystal with only van der Waals interactions between them, Fig. 8.

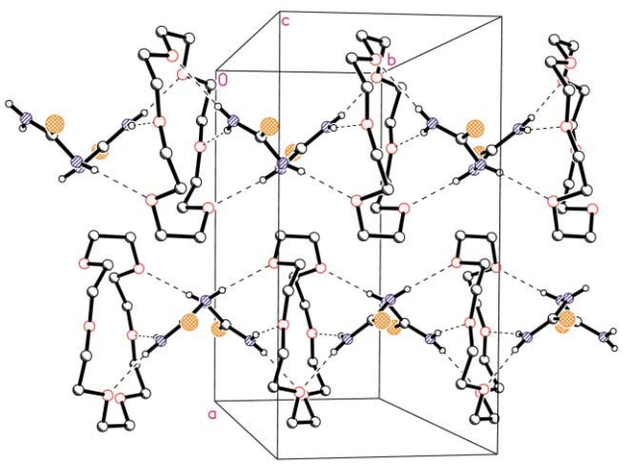

Fig. 8 Arrangement of chains in (**4**). Red: oxygens, blue: nitrogens, orange: sulfurs.

The organisation of (**5**) closely resembles (**4**) (Fig. 9). Each terminal amine group acts as H-donor in two H-bonds with the crown oxygens, N ··· O distances are N(1G) ··· O(4) 3.091(2), N(1G) ··· O(13) 3.213(3), and N(4G) ··· O4 (x, $y-1$, z) 2.941(2), N(4G) ··· O16 (x, $y-1$, z) 2.961(2) Å.

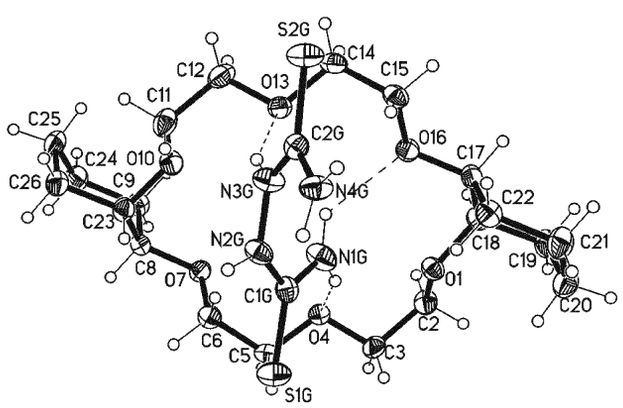

Fig. 9 ORTEP drawing for (**5**). The thermal ellipsoids are given with 50% probability level.

As in (**4**), two central amine groups of **dtur** molecule in a twisted mode are involved in short contacts with the crown spacer, N(3G) ··· O(13) 2.946(3), N(2G) ··· O(7) (x, $y-1$, z) 2.855(2) Å. Sustained by these N–H ··· O contacts, 1 : 1 polymeric chains, where DCHB and **dtur** molecules alternate, propagate in (**5**) along the b direction in the unit cell, Fig. 10.

To our knowledge, this is the first example of the close crystal structures for 18C6 and DCHB with the same organic molecule (complexes of 18C6 and DCHB with 4-amino-benzenesulfamide[16a,b] and with 6-chloro-7-sulfamido-3,4-dihydro-1,2,4-benzothiadiazine-1,1-dioxide[17a,b] afford different supramolecular architectures).

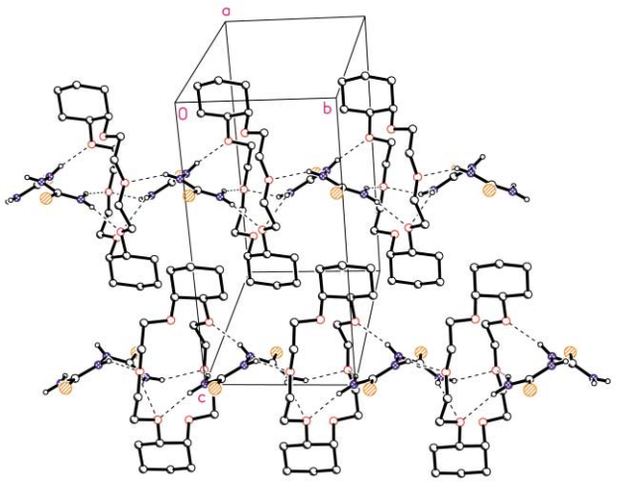

Fig. 10 Arrangement of chains in (**5**). Red: oxygens, blue: nitrogens, orange: sulfurs.

(**6**) crystallizes in the orthorhombic space group *Pbca* in a 1 : 2 ratio as shown in Fig. 11. The asymmetric unit contains a crown molecule, which sits on an inversion centre (with a probability of 50%) and a **dtur** molecule. Two **dtur** molecules approach each 15C5 molecule and the amine group defined by the N(1G) atom, participates in four N–H ··· O hydrogen bonds with the crown oxygens, the N ··· O separations are in the range 2.859(3)–3.093(3) Å (Table 1).

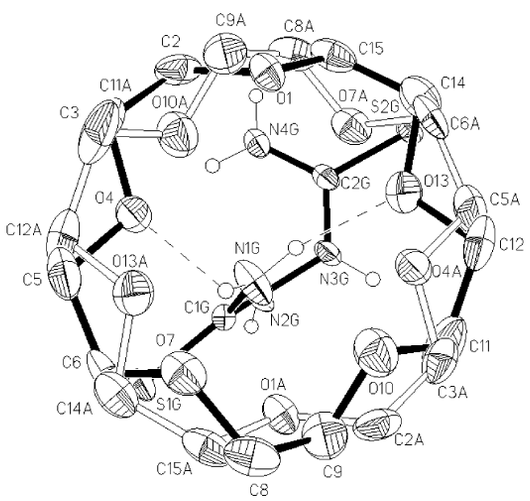

Fig. 11 ORTEP drawing for (**6**). The thermal ellipsoids are given with 30% probability level. Two positions (open and dark lines) for the 15C5 molecule are given. The centre-of-symmetry related **dtur** molecule is omitted.

The **dtur** molecules are self–assembled into pleated sheets that propagate parallel to the *ab* plane, Fig. 12. In the sheet each molecule is bound with four closest neighbours *via* N–H ··· S hydrogen bonds with three of four amine groups as H-donors and two sulfur atoms being involved in these interactions. The sheet is sustained by three different supramolecular synthons. Two secondary amine groups defined by the N(2G) and N(3G) atoms, form two similar planar supramolecular synthons, $R_2^2(8)$[18] between the molecules related by the glide plane, N(3G) ··· S(1G) ($-x+1/2$, $y-1/2$, z) 3.334(2), N(2G) ··· S(2G) ($-x+1/2$, $y+1/2$, z) 3.297(2) Å. Each synthon includes two different sulfur atoms and two secondary amine groups.[19] The same sulfur atoms are also involved in N–H ··· S hydrogen bonds with the primary amine group defined by the N(4G) atom, N(4G) ··· S(1G) ($-x$, $y-1/2$, $-z+1/2$) 3.396(2) Å and N(4G) ··· S(2G) ($-x$, $y+1/2$, $-z+1/2$) 3.464(1) Å, thus, the $R_4^2(9)$ synthon combines four **dtur**

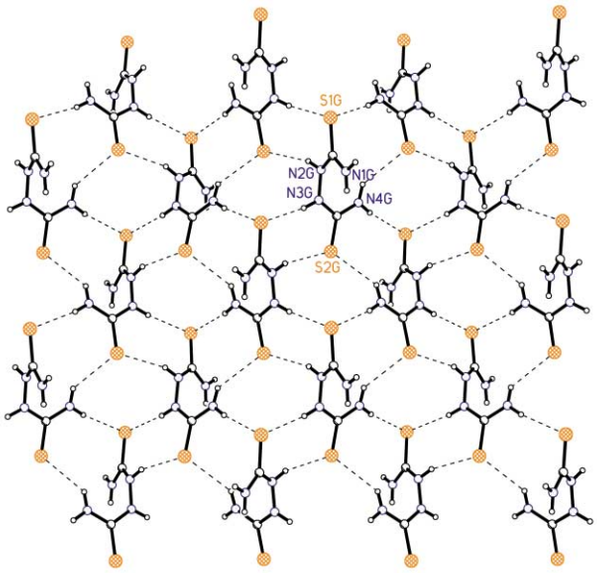

Fig. 12 View of the layer built of the **dtur** molecules in (**6**). Blue: nitrogens, orange: sulfurs.

molecules. In turn, each **dtur** molecule is engaged in four N–H ··· S hydrogen bonds within the sheet.

Sheets of **dtur** alternate with the sheets of 15C5 molecules along the *c* direction. The sheets are sustained by H-bonding to generate the three-dimensional grid illustrated in Fig. 13. To our knowledge, this is the first example of three-dimensional network that incorporates 15C5 molecules as the spacers between the layers of organic molecules.

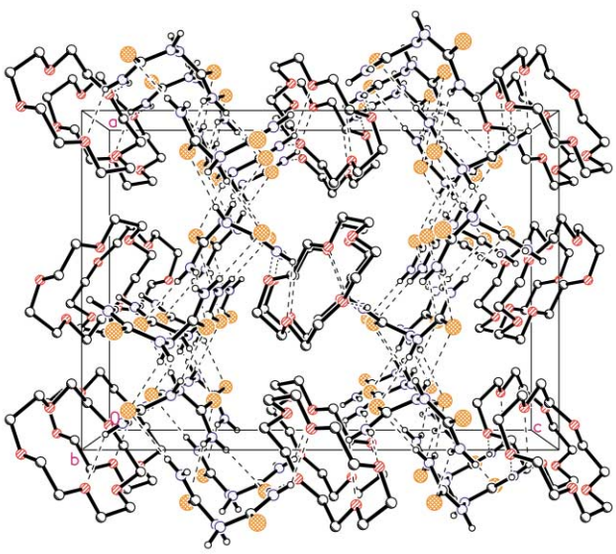

Fig. 13 Packing diagram for (**6**). Red: oxygens, blue: nitrogens, orange: sulfurs.

For the twinned crystal of (**7**) the asymmetric part of the monoclinic unit cell (space group $P2_1/c$) contains two 12C4 and two **dtur** molecules in general positions, and is depicted in Fig. 14.

Two 12C4 molecules are arranged in such a way that the dihedral angle between the mean planes through their oxygen atoms is equal to 30.80(4)°. Each primary amine group of **dtur** molecule acts as H-donor and forms two H-bonds with two crystallographically non-equivalent crown molecules, Fig. 14. Thus, each of two **dtur** molecules is joined *via* four single N–H ··· O hydrogen bonds with four crown molecules, related with the basic ones by inversion centres or translations. N ··· O distances fall in the range of 2.833(2)–2.991(2) Å for the **dtur** molecule containing the N(1G) atom and 2.860(2)–

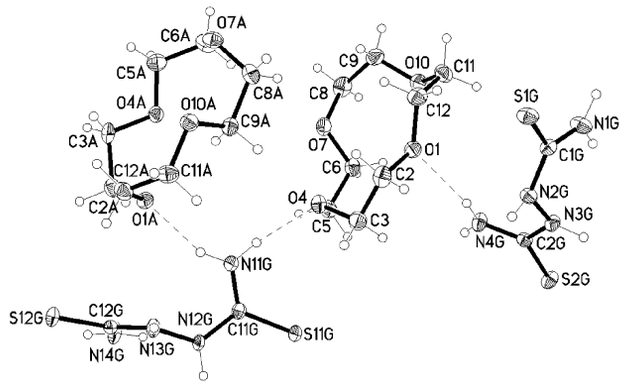

Fig. 14 ORTEP drawing for (**7**). The thermal ellipsoids are given with 30% probability level.

2.955(2) Å for the **dtur** molecule containing the N(11G) atom. Four molecules of 12C4 and 8 **dtur** molecules that belong to the adjacent chains are combined into centrosymmetric cages closed by 16 N–H ··· O hydrogen bonds, Fig. 15.

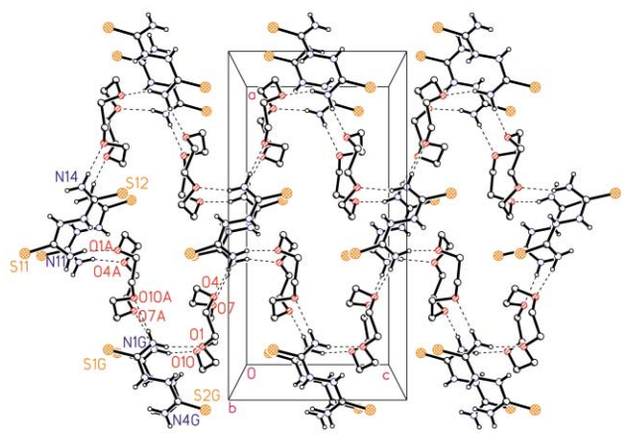

Fig. 15 Centrosymmetric cages closed by N–H ··· O hydrogen bonds in (**7**). The stacking **dtur** molecules belong to the neighbouring chains. Red: oxygens, blue: nitrogens, orange: sulfurs.

The crystallographically independent **dtur** molecules (defined by the S1G and S11G atoms), related by the glide plane, are consolidated into identical chains that alternate along the *a* direction in the unit cell. Two N–H ··· S hydrogen bonds N(2G) ··· S(2G) (x, $-y$ + 3/2, z + 1/2) 3.275(2) and N(3G) ··· S(1G) (x, $-y$ + 3/2, z − 1/2) 3.252(2) Å in one chain and N(12G) ··· S(12G) (x, $-y$ + 3/2, z − 1/2) 3.326(2) and N(13G) ··· S(11G) (x, $-y$ + 3/2, z + 1/2) 3.235(2) Å in another chain with participation of both central nitrogen atoms are responsible for the chain formation due to the $R_2^2(8)$ synthon,. The chains propagate along the *c* direction, Fig. 16.

In the *ab* plane the chains of **dtur** molecules of each type alternate with the rows of crown molecules attached to them. The closed cages are built of four crown molecules and two **dtur** molecules related by the inversion centre. In this layer (the second **dtur** molecule is removed to clarify the picture) the **dtur** molecules use all their proton-donor functionalities. A similar layer is formed with the participation of another **dtur** molecule and the same crown molecules. Due to the same crown connectors are involved in the both of these layers, the components in the crystal are consolidated into a three-dimensional grid where the identical **dtur** chains propagate along the *b* direction, while along the *a* direction these chains alternate, Fig. 17.

Conclusions

1. The dimensionality of the **dtox** molecule is a crucial factor that determines the close crystal packings in the complexes

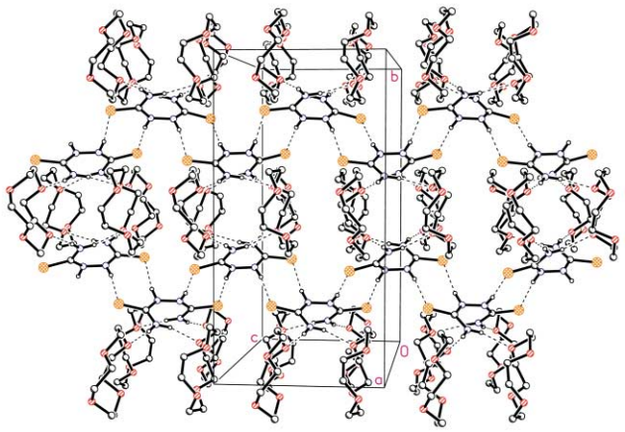

Fig. 16 Layer in (**7**) that combines one type of **dtur** molecules and crown ethers (the second type of **dtur** molecules is omitted). Red: oxygens, blue: nitrogens, orange: sulfurs.

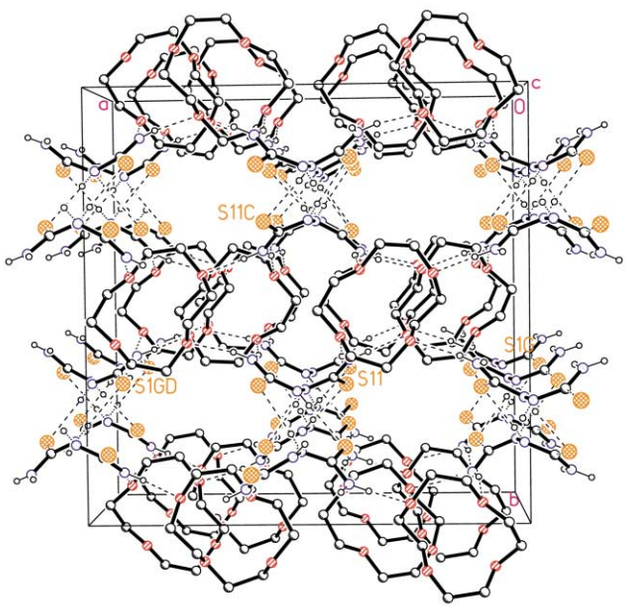

Fig. 17 Crystal packing for (**7**). Red: oxygens, blue: nitrogens, orange: sulfurs.

of 15-membered crown-ethers and diastereoisomers of dicyclohexyl-18-crown-6 in (**2**) and (**3**).

2. The size of 18-membered crown-rings of 18C6 and DCHB permits the accommodation of six NH ··· O hydrogen bonds and is a decisive factor for the similar crystal packings for (**4**) and (**5**).

3. The reduction of the crown ring in 15C5 and 12C4 explains the participation of only two (**6**) or one (**7**) proton of the amine group in NH ··· O crown interactions and the elaboration of another donor center in the **dtur** molecule for self-assembling and formulation of extended hydrogen-bonding networks in (**6**) and (**7**).

4. The melting points for two families of the compounds described being in the range of 160–180° for (**1**)–(**3**) and 230–240° for (**4**)–(**7**) reveal the direct relationship between the number of hydrogen bonds sustaining the two-component supramolecular architectures and the crystal stability.

5. The relative simplicity of these two model systems allow for specific interactions to be isolated and studied in the absence of the many other interactions available in natural biological systems.

Experimental

All the chemicals used (crown ethers, dithiooxamide and dithiobiurea) were purchased from Aldrich Chemical Co and were not purified prior to use. In all the experiments a 1 : 1 mixture of **dtox** or **dtur** (75 mg, 0.5 mmol) and 0.5 mmol of the corresponding crown ether was dissolved in a minimal amount (3 mL) of dimethylformamide at 100 °C and allowed to slowly evaporate. Crystals suitable for the X-ray diffraction experiments were isolated from the mass of crystals obtained. Suitable microanalyses were obtained for all compounds.

^{1}H and ^{13}C NMR spectra were obtained in DMSO-d_6 on a 250 MHz Bruker instrument. TGA data were obtained at a dynamic rate on a Hi-Res TGA 2950 thermogravimetric analyzer. All crystallographic measurements were carried out with a Nonius KappaCCD diffractometer equipped with graphite monochromated Mo-Kα radiation using ϖ rotations with sample-to-detector distance of 25 mm.

Red crystals of (**1**), mp 159–160 °C. Found, % C, 42.38; H, 7.14, N, 8.20 required for $C_{12}H_{24}N_2O_5S_2$: C, 42.33; H, 7.11; N, 8.23. TGA analysis shows that the complex decomposes in a single step at 169 °C (96.7%). ^{1}H NMR: δ = 10.18 (s, 2H, NH_2), 9.86 (s, 2H, NH_2), 3.52 (s, 20H, OCH_2). ^{13}C NMR: δ = 194.20 (*C*=S), 70.26 (O*C*H$_2$)

Crystal data for (**1**), triclinic, *P*-1, a = 8.266(5), b = 8.644(6), c = 12.532(1) Å, α = 80.05(3), β = 81.74(3), γ = 75.39(3)°, V = 848.7(1) Å^3, Z = 2, D_x = 1.332 g cm^{-3}, λ(Mo-Kα) 0.71073 Å, μ = 3.34 cm^{-1}, F(000) = 364, GoF = 1.122, R indices (all data) $R1$ = 0.1092, $wR2$ = 0.2389 for 2943 reflections and 245 parameters and R indices $R1$ = 0.0938, $wR2$ = 0.2308 for 2471 reflections obeying $I > 2\sigma(I)$ criterion of observability.

Red crystals of (**2**), mp 155–157 °C. Found, %: C, 47.08; H, 7.24; N, 9.19 required for $C_{24}H_{44}N_4O_6S_4$: C, 47.03; H, 7.27; N, 9.14. TGA analysis shows that the complex is stable to *ca.* 160–170 °C after which it decomposes in two steps at 177 °C (58.64%) and at 215 °C (40.95%). ^{1}H NMR: δ = 10.18 (s, 2H, NH_2), 9.59 (s, 2H, NH_2), 3.61–3.46 (m, 10H, OCH_2), 1.70 (d, 2H, CH_2), 1.46–1.21 (m, 6H, CH_2). ^{13}C NMR: δ = 194.46 (*C*=S), 76.84, 70.48, 67.89, 27.63, 22.01.

Crystal data for (**2**), monoclinic, *C*2/*c*, a = 23.720(1), b = 7.655(2), c = 18.364(3) Å, β = 106.98(6)°, V = 3189.1(1) Å^3, Z = 4, D_x = 1.276 g cm^{-3}, λ(Mo-Kα) 0.71073 Å, μ = 3.39 cm^{-1}, F(000) = 1312, GoF = 1.067, R indices (all data) $R1$ = 0.0582, $wR2$ = 0.1033 for 3649 reflections and 198 parameters and R indices $R1$ = 0.0424, $wR2$ = 0.0966 for 3033 reflections obeying $I > 2\sigma(I)$ criterion of observability.

Red crystals of (**3**), mp 179–180 °C, Found, %: C, 47.10; H, 7.28; N, 9.10; required for $C_{24}H_{44}N_4O_6S_4$: C, 47.03; H, 7.27; N, 9.14. TGA analysis shows that the complex decomposes in two steps at 173 °C (50.50%) and 207 °C (49.64%). ^{1}H NMR: δ = 10.18 (s, 2H, NH_2), 9.59 (s, 2H, NH_2), 3.61–3.46 (m, 10H, OCH_2), 1.70 (d, 2H, CH_2), 1.44–1.19 (m, 6H, CH_2). ^{13}C NMR: δ = 194.46 (*C*=S), 76.84, 70.48, 67.89, 27.63, 22.01.

Crystal data for (**3**), monoclinic, $P2_1/n$, a = 12.654(3), b = 7.570(2), c = 17.129(3) Å, β = 106.14(3)°, V = 1576.1(5) Å^3, Z = 2, D_x = 1.291 g cm^{-3}, λ(Mo-Kα) 0.71073 Å, μ = 3.43 cm^{-1}, F(000) = 656, GoF = 1.097, R indices (all data) $R1$ = 0.0494, $wR2$ = 0.1144 for 3592 reflections and 184 parameters and R indices $R1$ = 0.0421, $wR2$ = 0.1103 for 3212 reflections obeying $I > 2\sigma(I)$ criterion of observability.

Colorless needles of (**4**), mp 228–230 °C. Found, %: C, 40.61, H, 7.26, N, 13.59; required for $C_{14}H_{30}N_4O_6S_2$: C, 40.56, H, 7.29, N, 13.52. TGA analysis shows a complex multiple weight losses at 152.44 °C (29.05%), 199.37 °C (61.36%) and 613.23 °C (9.303%).

Crystal data for (**4**), monoclinic, $P2_1/c$, a = 14.196(3), b = 7.187(2), c = 19.552(3) Å, β = 92.18(2)°, V = 1993.4(8) Å^3, Z = 4, D_x = 1.381 g cm^{-3}, λ(Mo-Kα) 0.71073 Å, μ = 3.04 cm^{-1}, F(000) = 888, GoF = 1.023, R indices (all data) $R1$ = 0.0452, $wR2$ = 0.0782 for 4532 reflections and 259 parameters and R indices $R1$ = 0.0334, $wR2$ = 0.0748 for 3860 reflections obeying $I > 2\sigma(I)$ criterion of observability.

Colorless needles of (**5**), mp 226–228 °C. Found, %: C, 50.53, H, 8.17, N, 10.75; required for $C_{22}H_{42}N_4O_6S_2$: C, 50.55, H, 8.10, N, 10.72%. ^{1}H NMR: δ = 9.50 (s, 2H, NH–NH), 8.45 (s, 4H, –NH_2), 3.60 (s, 16H, –CH_2O); ^{13}C NMR: δ = 183.20 (C=S), 70.25 (CH_2O).

Crystal data for (**5**), monoclinic, *Pn*, a = 12.489(2), b = 7.509(2), c = 14.639(3) Å, β = 93.61(3)°, V = 1370.1(5) Å^3, Z = 2, D_x = 1.267 g cm^{-3}, λ(Mo-Kα) 0.71073 Å, μ = 2.36 cm^{-1}, F(000) = 564, GoF = 1.067, R indices (all data) $R1$ = 0.0315, $wR2$ = 0.0796 for 3097 reflections and 331 parameters and R indices $R1$ = 0.0303, $wR2$ = 0.0789 for 3019 reflections obeying $I > 2\sigma(I)$ criterion of observability.

Colorless needles of (**6**), mp 235–237 °C, Found, %: C, 32.25, H, 6.23, N, 21.61, required for $C_{14}H_{32}N_8O_5S_4$: C, 32.29, H, 6.19, N, 21.52.

TGA analysis indicates that the host decomposes at 187 °C (44.72 %) followed by multiple weight losses for the guest at 204.24 °C (25.06%), 280.83 °C (15.40%), and 585.60 °C (14.82%); ^{1}H NMR: δ = 9.34 (s, 2H, N*H*–N*H*), 8.01 (broad s, 2H, NH_2), 7.20 (broad s, 2H, NH_2), 3.52 (s, 10H, OCH_2); ^{13}C NMR: δ = 180.24 (*C*=S), 70.13 (O*C*H$_2$)

Crystal data for (**6**), orthorhombic, *Pbca*, a = 13.632(3), b = 9.475(2), c = 19.185(4) Å, V = 2478.0(9) Å^3, Z = 4, D_x = 1.396 g cm^{-3}, λ(Mo-Kα) 0.71073 Å, μ = 4.24 cm^{-1}, F(000) = 1104, GoF = 1.079, R indices (all data) $R1$ = 0.0519, $wR2$ = 0.0971 for 3579 reflections and 232 parameters and R indices $R1$ = 0.0411, $wR2$ = 0.0917 for 3158 reflections obeying $I > 2\sigma(I)$ criterion of observability.

Colorless needles of (**7**), mp 235–237 °C, Found, %: C, 36.76, H, 6.84, N, 17.21, required for $C_{10}H_{22}N_4O_4S_2$: C, 36.79, H, 6.79, N, 17.16. TGA analysis indicates that the host decomposes at 132.60 °C (53.25%), followed by multiple weight losses for the guest at 218.70 °C (26.88%), 314.16 °C (7.437%), 594.52 °C (12.14%); ^{1}H NMR: δ = 9.30 (s, 2H, NH–NH), 7.92 (s, 2H, NH_2), 7.26 (s, 2H, NH_2); ^{13}C NMR: δ = 182.77 (C=S), 70.312 (CH_2O).

Crystal data for (**7**), monoclinic, $P2_1/c$, a = 18.475(4), b = 18.445(4), c = 9.443(2) Å, β = 90.00(3)°, V = 3217.9(12) Å^3, Z = 8, D_x = 1.348 g cm^{-3}, λ(Mo-Kα) 0.71073 Å, μ = 3.48 cm^{-1}, F(000) = 1392, GoF = 0.926, R indices (all data) $R1$ = 0.0448, $wR2$ = 0.0828 for 9354 reflections and 404 parameters and R indices $R1$ = 0.0343, $wR2$ = 0.07 for 8171 reflections obeying $I > 2\sigma(I)$ criterion of observability.

Tables of crystal data, atomic coordinates and thermal parameters, full bond distances and angles, and structure factors may be obtained on request from the authors. CCDC reference numbers 202644–202650 for compounds (**1**)–(**7**), respectively.

See http://www.rsc.org/suppdata/ob/b3/b301379k/ for crystallographic data in CIF or other electronic format.

Acknowledgements

Support of this research from MRDA (Moldova)–CRDF (USA) (grant MP2-3021) is gratefully acknowledged.

References

1 B. Moulton and M. J. Zaworotko, *Chem. Rev.*, 2001, **101**, 1629–1658.
2 (*a*) G. M. J. Schmidt, *Pure Appl. Chem.*, 1971, **27**, 647–678; (*b*) G. R. Desiraju, *Crystal Engineering: the Design of Organic Solids*, Elsevier, Amsterdam, 1989.
3 G. R. Desiraju, *Angew. Chem., Int. Ed. Engl.*, 1995, **34**, 2311–2327.
4 E. Boucher, M. Simard and J. D. Wuest, *J. Org. Chem.*, 1995, **60**, 1408–1412.
5 (*a*) M. J. Zaworotko, *Chem. Soc. Rev.*, 1994, **23**, 283–288; (*b*) C. V. K. Sharma and M. J. Zaworotko, *Chem. Commun.*, 1996, 2655–2656.
6 R. Feynman, *Eng. Sci.*, 1960, 22–36.
7 (*a*) Yu. A. Simonov, M. S. Fonari, V. Ch. Kravtsov, J. Lipkowski, E. V. Ganin and A. A. Yavolovskii, *Crystallogr. Rep. (Transl. Kristallografiya)*, 2002, **47/1**, 86–93; (*b*) M. S. Fonari, Yu. A. Simonov, V. Ch. Kravtsov, J. Lipkowski, E. V. Ganin and A. A. Yavolovskii, *J. Mol. Struct.*, 2003, **647**(1–3), 129–140.
8 F. H. Allen, *Acta Crystallogr., Sect. B*, 2002, **58**, 380–388.
9 For information about 12-crown-4 complexes with neutral molecules see: (*a*) O. Moers, K. Wijaya, P. G. Jones and A. Blaschette, *Acta Crystallogr., Sect. C (Cr. Str. Comm.)*, 1999, **55**, 1542–1545; (*b*) K. Wijaya, O. Moers, P. G. Jones and A. Blaschette, *Acta Crystallogr., Sect. C: Cryst. Struct. Commun.*, 1998, **54**, 818–820; (*c*) E. A. Babaian, M. Huff, F. A. Tibbals and D. C. Hrncir, *Chem. Commun.*, 1990, 306–307; (*d*) Yu. A. Simonov, M. S. Fonari, A. A. Dvorkin, T. I. Malinovskii, J. Lipkowski and E. V. Ganin, *J. Inclusion Phenom. Macrocyclic Chem.*, 1993, **16**, 315–327; (*e*) A. Michalides, D. Henschel, A. Blaschette and P. G. Jones, *Z. Naturforsch., B*, 1995, **50**, 1018–1024.
10 For information about 15-crown-5 complexes with neutral molecules see: (*a*) A. A. Dvorkin, Yu. A. Simonov, K. Suwinska, J. Lipkowski, T. I. Malinowski, E. V. Ganin and S. A. Kotlyar, *Kristallografiya*, 1991, **36**, 62–69; (*b*) W. H. Watson and P. C. Jain, *J. Inclusion Phenom.*, 1986, **4**, 397–405; (*c*) R. Luboradzki, J. Lipkowski, Yu. A. Simonov, M. S. Fonari, E. V. Ganin and A. A. Yavolovskii, *J. Inclusion Phenom.*, 2001, **40**, 59–65.
11 (*a*) S. Harkema, G. J. Hummel, K. Daasvatn and D. N. Reinhhoudt, *J. Chem. Soc., Chem. Commun.*, 1981, 368–370; (*b*) G. Weber, *J. Inclusion Phenom.*, 1984, **1**, 339–345; (*c*) M. G. B. Drew and D. G. Nicholson, *Acta Crystallogr., Sect. C*, 1985, **1**, 1358–1360; (*d*) G. Weber, *Acta Crystallogr., Sect. C*, 1983, **39**, 896–899; (*e*) I. Goldberg, *Crown Ethers and Analogs*, John Wiley, 1989, ch. 7, pp. 399–476.
12 P. J. Weatley, *J. Chem. Soc.*, 1965, 396–400.
13 A. Pignedoli, G. Peyronel and L. Antolini, *Acta Crystallogr., Sect. B*, 1975, **31**, 1903–1906.
14 W. H. Watson, J. Galloy, D. A. Grossie, F. Vögtle and W. M. Müller, *J. Org. Chem.*, 1984, **49**, 347–352.
15 For information about dicyclohexyl-18-crown-6 complexes with neutral molecules see: (*a*) Junior J. R. Damewood, J. J. Urban, T. C. Williamson and A. L. Rheingold, *J. Org. Chem.*, 1988, **53**, 167–171; (*b*) M. S. Fonar, Yu. A. Simonov, A. A. Dvorkin, T. I. Malinowsky, E. V. Ganin, S. A. Kotlyar and V. F. Makarov, *J. Inclusion Phenom. Macrocyclic Chem.*, 1989, **7**, 613–622; (*c*) A. A. Dvorkin, M. S. Fonar, E. V. Ganin, Yu. A. Simonov and G. S. Musienko, *Kristallografiya*, 1991, **36**, 70–76; (*d*) Yu. A. Simonov, M. S. Fonar, K. Suwinska, A. A. Dvorkin, A. N. Sobolev, E. V. Ganin and N. G. Luk'yanenko, *Kristallografiya*, 1992, **37**, 900–908; (*e*) Yu. Simonov, L. P. Battaglia, A. Corradi, S. Ianelli, G. Pelosi, E. Ganin and N. Lukjanenko, *J. Inclusion Phenom. Macrocyclic Chem.*, 1990, **9**, 181–194; (*f*) Yu. A. Simonov, T. I. Malinowskii, E. V. Ganin, S. A. Kotlyar, G. Bocelli, G. Calestani and C. Rizzoli, *J. Inclusion Phenom. Macrocyclic Chem.*, 1990, **8**, 349–361.
16 (*a*) S. T. Malinowski, E. V. Ganin, Yu. A. Simonov and V. F. Makarov, *Izv. Akad. Nauk Mold. SSR., Ser. Fiz.–Tekh. Mat. Nauk.*, 1989, **1**, 23–26; (*b*) A. A. Dvorkin, M. S. Fonari, S. T. Malinowski, E. V. Ganin, Yu. A. Simonov, V. F. Makarov, S. A. Kotlyar and N. G. Lukyanenko, *Zh. Strukt. Khim.*, 1989, **30**, 96–101.
17 (*a*) A. A. Dvorkin, Yu. A. Simonov, J. Lipkowski, M. S. Fonari, T. I. Malinowski, E. V. Ganin and S. A. Kotlyar, *Kristallografiya*, 1990, **35**, 682–686; (*b*) Yu. A. Simonov, M. S. Fonari, G. Bocelli, G. Calestani, J. Lipkowski, K. Suwinska and E. V. Ganin, *Supramol. Chem.*, 1995, **4**, 251–258.
18 For information about graph–set notation see: (*a*) J. Bernstein, R. E. Davis, L. Shimoni and N.-L. Chang, *Angew. Chem., Int. Ed. Engl.*, 1995, **34**, 1555–1573; (*b*) M. C. Etter, *Acc. Chem. Res.*, 1990, **23**, 120–126.
19 For some recent examples of $R_2^2(8)$ NH $\cdots$ S synthon in thiosemicarbazides see: (*a*) G. H. W. Rabe, R. Roesky, H.-G. Bohra, G. M. J. Schmidt and M. Noltemeyer, *J. Fluorine Chem.*, 1991, **52**, 235–244; (*b*) B. J. Childs, J. M. Cadogan, D. C. Craig, M. L. Scudder and H. A. Goodwin, *Aust. J. Chem.*, 1998, **51**, 273–284; (*c*) V. N. Nesterov, A. M. Shestopalov, Yu. A. Sharanin, I. A. Aitov, V. E. Shklover, Yu. T. Struchkov and V. P. Litvinov, *Izv. Akad. Nauk SSR, Ser. Khim.*, 1991, 896–902; (*d*) D. Kaiser, G. Videnov, C. Maichle-Mossmer and J. G. Jung Strahle, *J. Chem. Soc., Perkin Trans. 2*, 2000, 1081–1085; (*e*) M. L. B. F. Hereygers, H. O. Desseyn, S. P. Perlepes, K. A. F. Verhulst and A. T. H. Lenstra, *J. Chem. Crystallogr.*, 1995, **25**, 181–187.